Nonlinear regime operation for a high resolution vibrating beam UGS seismometer

Raphaël Levy, Guillaume Papin, Olivier Le Traon, Denis Janiaud, Jean Guérard

Nonlinear regime operation for a high resolution vibrating beam UGS seismometer

Raphael Levy · Guillaume Papin · Olivier Le Traon · Denis Janiaud · J. Guerard

Abstract MEMS vibrating beam accelerometers use the variation of frequency of a vibrating beam attached to a proof mass to measure its applied acceleration. Considering inertial navigation applications, the beam is actuated in the linear regime to keep high eigen frequency stability. Concerning the new application of MEMS accelerometers as UGS seismometers, the bias stability is not important anymore and the important parameter is the resolution at integration time of 1 ms. It becomes then interesting to actuate the beam in the nonlinear regime. This paper presents a behavioral model of the vibrating beam accelerometer including the nonlinear terms. This model is validated by experimental measurements and phase noise in the nonlinear regime is simulated. The seismometer resolution is then calculated in the nonlinear regime and compared to other state of the art UGS seismometers.

Keywords Accelerometer · Seismometer · Nonlinear resonator · Phase noise

1 Introduction

1.1 Application of MEMS accelerometers to seismic UGS (unattented ground sensor) applications

Seismometers have been widely used for earthquake monitoring and oil & gas prospecting. More recently, seismometers have been integrated in wireless sensors networks for areas surveillance. The goal of the seismometers used as unattended ground sensors (UGS) is to detect and identify walking persons or moving vehicles by means of seismic waves measurements [1–4]. The bandwidth of the seismic signal is from DC to 1,000 Hz.

The small size and low power consumption of MEMS accelerometers allows using them in such applications. Their advantages over the conventional geophones are the following [5, 6]: the MEMS accelerometer is DC coupled whereas the geophone acts as a high pass filter and signal below 10 Hz is not detected, it is also much smaller and more robust to shocks, while showing a good signal to noise ratio.

Figure 1 shows such a ground acceleration measurement produced by a walking person and measured by state of the art accelerometer. The amplitude of the acceleration sine wave is measured and related to the distance of the person to the sensor, so the bias stability is not important in this application whereas the resolution is critical as it determines the maximum distance of detection.

1.2 The high resolution vibrating beam seismometer

The vibrating beam accelerometer (VBA) consists in a vibrating micro beam anchored on one side and linked to a proof mass on the other side as shown in Fig. 2. The beam is maintained at resonance by means of an oscillator circuit, and when the proof mass is submitted to acceleration, compressive or tensile stresses are applied on the vibrating beam modifying its resonance frequency. The output of the accelerometer is a frequency measurement, its resolution is determined by the phase noise integrated over the sensor bandwidth, and its bias stability is determined by the close to carrier phase noise or frequency stability.

The high resolution VBA developed at ONERA [7] is presented in Fig. 2. Its acceleration noise expressed as the Allan deviation over integration time is presented in Fig. 3. This acceleration noise shows a low noise $<$100 ng for

R. Levy (✉) · G. Papin · O. Le Traon · D. Janiaud · J. Guerard
Physics and Instrumentation Department, ONERA, Châtillon, France
e-mail: raphael.levy@onera.fr

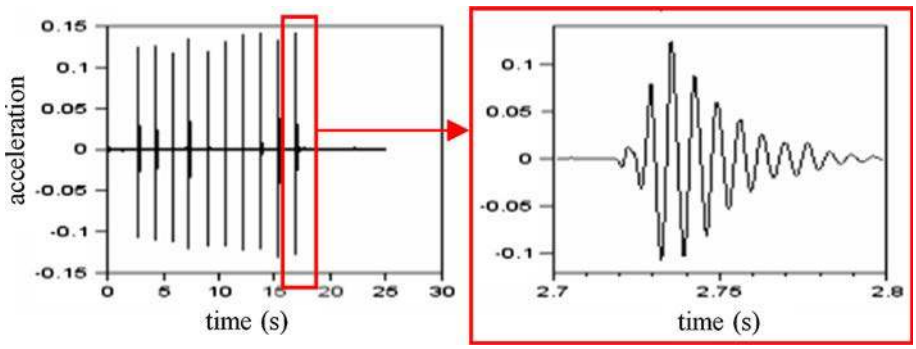

Fig. 1 Ground acceleration measurement showing the seismic waves produced by a walking person: on the left each spike corresponds to a footstep, on the right the ground acceleration in response to a footstep is shown

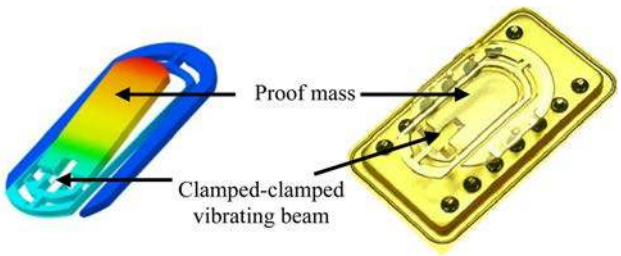

Fig. 2 On the left finite element model of the vibrating beam accelerometer showing the vibrating beam attached to the proof mass. The manufactured quartz crystal accelerometer structure is presented on the *right*

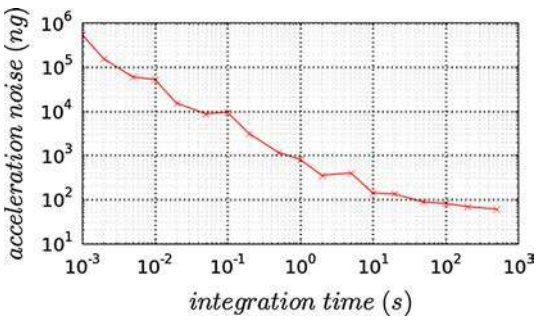

Fig. 3 Acceleration noise of the high resolution VBA expressed as the Allan deviation over integration time

integration time >30 s but higher noise for integration time of 1 ms used for UGS applications. This acceleration noise measurement has been performed while operating the beam resonator in the linear regime, the goal of this work is to quantify the achievable reduction of noise obtained by operating the vibrating beam in the nonlinear regime. Towards that purpose, the behavioral model of the VBA including nonlinear terms is presented, and then phase noise simulations are performed and analyzed.

1.3 Phase noise in the nonlinear regime

Recent works [8] have investigated the phase noise of an oscillator including nonlinear terms. They show that, in presence of mechanical nonlinear terms of the resonator, increasing the amplitude of the excitation force leads to an improvement of the far from carrier phase noise and a degradation of the close to carrier phase noise. Concerning the vibrating beam accelerometer, the excitation amplitude increase leads to the decrease of the accelerometer noise over a high bandwidth at the cost of a decrease of the bias stability, this is not recommended for inertial application where the acceleration is twice integrated but is interesting for seismic ground sensor applications where bias stability is not considered and the important parameter is the resolution at the bandwidth determined by the frequency of the seismic waves ($\sim$DC-1,000 Hz). In this case it is then better to operate the beam resonator in the nonlinear regime to improve the sensor resolution and thus the maximum detection distance.

The development of a behavioral model of the nonlinear resonator and its oscillator electronics and its phase noise simulation has permitted the optimization of the VBA in the nonlinear regime. These models, simulations and experimental measurements are presented in this paper.

2 Behavioural modeling of the oscillator

2.1 Behavioral oscillator model

The behavioral model of the VBA shown in Fig. 4 has been presented in previous papers [9, 10], it includes:

- The mass & stiffness resonator model equation including the Duffing mechanical nonlinear term:

$$F_x = m\ddot{x} + d\dot{x} + kx + k_3x^3 \quad (1)$$

F_x: actuation force (N), x: displacement (m), m: equivalent mass (kg), d: damping term (kg/s), k: equivalent stiffness (N/m), k_3: nonlinear stiffness (N/m^3).

For a clamped–clamped beam, the parameters of Eq. 1 can be expressed with the parameters of the beam. Details of the calculations can be found in [11]:

$$k = \frac{16Ehe^3}{L^3} \quad (2)$$

$$m = 0.38\rho ehL \quad (3)$$

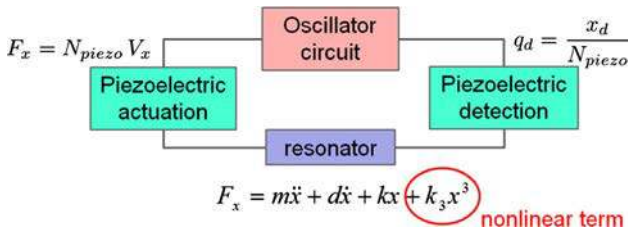

Fig. 4 Behavioural model of the quartz crystal MEMS oscillator including the mechanical cubic nonlinear term

$$d = \frac{m\omega_0}{Q} \tag{4}$$

E: quartz Young modulus (Pa), ρ: quartz density (kg/m^3), h: height of the beam (m), e: width of the beam (m), L: length of the beam (m), ω_0: eigen frequency of the beam, Q: quality factor of the beam.

The eigen frequency for a clamped–clamped beam is shown in Eq. 5. Details of the calculation can be found in [12]:

$$\omega_0 = \frac{3.52}{2\sqrt{3}} \frac{e}{L^2} \sqrt{\frac{E}{\rho}} \tag{5}$$

The damping term of the beam is limited by thermoelsatic damping, its quality factor is derived in [13, 14]:

$$Q = \frac{\rho Cp(f_0^2 + f_t^2)}{\alpha^2 T_0 E f_0 f_t} \quad f_t = \frac{\rho K_t}{2\rho C_p e^2} \tag{6}$$

Kt: quartz thermal conductibility (W m^{-1} K^{-1}), Cp: quartz heat capacity at constant pressure (J kg^{-1} K^{-1}), α: thermal expansion coefficient (K^{-1}).

The expression of the Duffing nonlinear stiffness term is calculated in [11]:

$$k_3 = \frac{k}{\sqrt{2}e^2} \tag{7}$$

- The linear piezoelectric transduction equation:

$$F_x = N_{piezo} V_x \tag{8}$$

$$q = N_{piezo} X \tag{9}$$

$$N_{piezo} = e_{12} \frac{3eh}{L} \tag{10}$$

N_{piezo} is the linear piezoelectric transduction parameter (C/m), F_x is the excitation force (N), V_x is the excitation voltage (V), q are the electric charges (C), X the mechanical displacement (m), e_{12} is the piezoelectric coefficient (N V^{-1} m^{-1}).

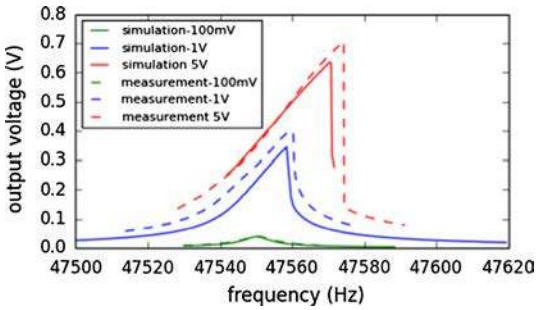

Fig. 5 Experimental and simulations based nonlinear resonance curves for the quartz clamped–clamped resonator of the vibrating beam accelerometer

As piezoelectric transduction remains linear, the main nonlinearity originates from the resonator.

- The analog electronics self-sustained oscillator. The components of the circuit are described by their spice model including the associated white and flicker noise sources.

2.2 Open loop model simulation

Transient open loop simulations are performed on the mechanical resonator including piezoelectric transduction and compared to experimental measurements on the accelerometer quartz resonator: the experimental setup consists in a waveform generator to actuate the resonator, a charge amplifier at the resonator output that output voltage is proportional to the mechanical displacement of the cantilever. The actuation frequency is swept around the eigen frequency, and the resonance curve is repeated for three values of the excitation voltage. The results are shown in Fig. 5 and show nonlinear behavior in good agreement between measurements and simulations, this validates that the main nonlinear term originates from the mechanical resonator nonlinear term in Eq. 1.

2.3 Phase noise simulation

Closed loop simulations can then be performed including the resonator and the self-sustained oscillator circuit models.

Phase noise can be simulated once the steady state is reached with the Pnoise tool of the cadence software. This phase noise is then used to calculate the Allan deviation that is a standard measurement of noise for sensors. The Allan deviation for an integration time of 1 ms is then the parameter to optimize to design a high resolution UGS seismometer.

3 Optimization of the UGS seismometer resolution

3.1 From phase noise to acceleration noise

Once the phase noise of the accelerometer has been simulated, in order to obtain the resolution of the accelerometer integrated over its bandwidth, the phase noise is converted into frequency noise, and then into acceleration noise expressed as the Allan deviation that is a standard performance measurement for sensors.

The phase noise $S_\Phi(f)$ is expressed in dBc/Hz as the spectral density of a signal's phase deviation where f is the relative frequency from the carrier. It can be simulated by Cadence software given a behavioral model of the resonator, the piezoelectric transduction model, and the oscillator circuit model. A Periodic steady state simulation is first performed, followed by a phase noise simulation.

This phase noise can be converted into frequency noise [15]:

$$S_y(f) = \frac{f^2}{f_0^2} S_\varphi(f) \tag{11}$$

The frequency noise is then converted into the Allan frequency deviation [15]:

$$\sigma_y^2(\tau) = 2 \int_0^\infty S_y(f) \frac{\sin^4(\pi\tau f)}{(\pi\tau f)^2} df \tag{12}$$

Finally the Allan frequency deviation is converted into Allan acceleration deviation expressed in g:

$$\sigma_A(\tau) = \sigma_y(\tau) K \tag{13}$$

where K is the accelerometer scale factor (Hz/g).

3.2 VBA acceleration noise in the nonlinear regime

The Allan deviation is simulated for increasing values of the excitation voltages as shown in Figs. 6 and 7. It shows that increasing the excitation voltage:

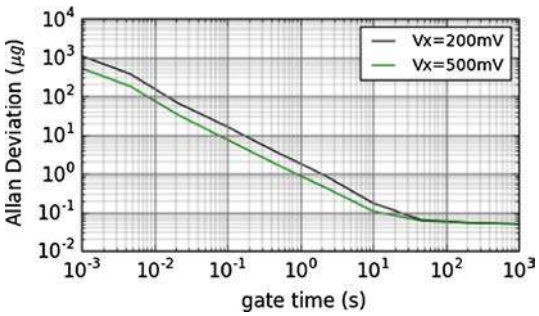

Fig. 6 Allan acceleration deviation for increasing values of the excitation voltage remaining in the linear regime

– In the linear regime ($V_x < 500$ mV):
  - Improves noise at an integration time of 1 ms
  - Has no impact on noise at high integration times
– In the nonlinear regime ($V_x > 500$ mV):
  - Improves noise at an integration time of 1 ms
  - Worsens noise at high integration times

3.3 Application to the vibrating beam UGS seismometer

Concerning seismic ground sensor applications where the bias stability is not considered and the important parameter is the sensor resolution at an integration time of 1 ms, it is better to actuate the resonator in the nonlinear regime. Actuating the resonator with a 8 V excitation voltage leads to a resolution of 50 µg. This VBA resolution makes it a good UGS seismometer compared to state of the art MEMS UGS seismometers as shown in Table 1. Compared to the other silicon MEMS pendular accelerometers presented in Table 1, the VBA has the advantage of a direct digital frequency output that allows a wide dynamic range and no need for ADC, there is also no need for high polarization voltage (piezoelectric transduction), and a good tradeoff between resolution and power consumption.

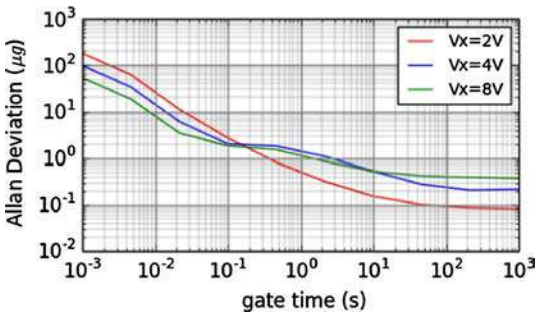

Fig. 7 Allan acceleration deviation for increasing values of the excitation voltage in the nonlinear regime

Table 1 Performances of state of the art MEMS seismometers used as UGS for area surveillance

MEMS accelerometer	Resolution @ 1 ms integration time (µg)	Power consumption (mW)
SD1221 [16]	150	25
SF1500 [17]	10	150
VBA (this work)	40	50

3.4 Application to the vibrating beam accelerometer for inertial navigation

For other applications of vibrating beam accelerometers such as inertial navigation, the acceleration measurement is twice integrated to calculate the position, and as a consequence the bias stability is crucial. The bias stability is deteriorated when the beam resonator operates in the nonlinear regime, this is the reason why VBAs work in the linear region for inertial applications.

4 Conclusions

The acceleration noise simulation of the VBA has been performed with an excitation voltage high enough to drive the clamped–clamped beam resonator in the nonlinear regime. It shows, in the nonlinear regime, an improvement of the resolution at low integration time but worsens the resolution for higher integration time. It is thus interesting to actuate the resonator in the nonlinear regime for seismic ground sensor applications where the dynamic acceleration is measured and the resolution at integration time of 1 ms determines the maximum distance of detection. If excited in the nonlinear regime, the resolution of the VBA can be as good as 50 μg at integration time of 1 ms, that design is well suited for UGS seismometer application.

References

1. Sabatier, J. M., Ekimov, A. E., (2008). "A review of human signatures in urban environments using seismic and acoustic methods". *IEEE Conference on* technologies for homeland security, 215–220.
2. Mehmood, A., Patel, V. M., Damarla, T., (2012). "Discrimination of bipeds from quadrupeds using seismic footstep signatures". *2012 IEEE International Geoscience and Remote Sensing Symposium (IGARSS)*, 6920–6923.
3. Sharif, H., et al. (2004). An efficient and robust approach to vehicule classification using wavelet domain seismic signal processing in IEEE.
4. Mehmood, A., et al. (2012). Discrimination of bipeds from quadrupeds using seismic footsteps signature in IEEE.
5. HONS, M., et al. (2007). Ground motion through geophones and MEMS accelerometers: sensors comparison in theory, modelling and field data.
6. Speller, K. E., Duli, Yu. (2004). "A low noise MEMS accelerometer for unattended ground sensor application". Proc. SPIE 5417, Unattended/Unmanned Ground, Ocean, and Air Sensor Technologies and Applications VI, 63. doi:10.1117/12.540337.
7. Levy, R., Janiaud, D.; Guerard, J., Taibi, R., Le Traon, O., (2014). "A 50 nano-g resolution quartz Vibrating Beam Accelerometer". *International Symposium on Inertial Sensors and Systems (ISISS)*.
8. He, L., (2010). "A state-space phase noise model for nonlinear MEMS oscillators employing automatic amplitude control". *IEEE Transactions on Circuits and Systems*, 189–199.
9. Papin, G. (2012). "Behavioural modelling of MEMS oscillators and phase noise simulation". *Journal of Analog Integrated Circuits and Signal Processing, 72*, 11–18.
10. Levy, R., (2010). "Phase noise analysis and performance of the vibrating beam accelerometer". *IEEE Requency Control Symposium*.
11. Kaajakari, V., Mattila, T., Oja, A., & Seppa, H. (2004). Nonlinear limits for single-crystal silicon microresonator, microelectromechanical systems. *Journal of, 13*(5), 715–724.
12. Morse, P. M., Ingard, K. U., (1968). Theoretical Acoustics, McGraw-Hill, 467–468.
13. Zener, C. (1937). Internal friction in solids i : theory of internal friction in reeds. *Physical Review, 52*, 230–235.
14. Zener, C. (1938). Internal friction in solids ii : general theory of thermoelastic internal friction. *Physical Review, 53*, 90–99.
15. Rubiola, E., (2008). "Phase Noise and Frequency Stability in Oscillators", Cambridge university press. The Cambridge RF and Microwave Engineering Series. isbn: 9780521886772.
16. JO, H.,, Rice,J. A., et al. (2010). "Development of a High-sensitivity Accelerometer Board for Structural Health Monitoring", sensors and smart structures technologies for civil, mechanical, and aerospace systems 2010. *Proceedings of SPIE*, 7647.
17. COLIBRYS application note n°30N.UGS.B.05.11, Seismic accelerometers for unattended ground sensors (UGS).